

**Please cite the Published Version**

Faghand, E, Karimian, S, Mehrshahi, E and Karimian, N (2021) Couplinor: a simple computational tool for synthesis of multi-section coupled-line filter based on MPCM-TLM technique. International Journal of Microwave and Wireless Technologies, 13 (9). pp. 887-896. ISSN 1759-0787

**DOI:** <https://doi.org/10.1017/s1759078721000167>

**Publisher:** Cambridge University Press (CUP)

**Version:** Accepted Version

**Downloaded from:** <https://e-space.mmu.ac.uk/627380/>

**Usage rights:** © In Copyright

**Additional Information:** Copyright The Author(s), 2021. Published by Cambridge University Press in association with the European Microwave Association.

**Enquiries:**

If you have questions about this document, contact [openresearch@mmu.ac.uk](mailto:openresearch@mmu.ac.uk). Please include the URL of the record in e-space. If you believe that your, or a third party's rights have been compromised through this document please see our Take Down policy (available from <https://www.mmu.ac.uk/library/using-the-library/policies-and-guidelines>)

# Couplicator: A New Simple Tool for Design of Multi-Section Coupled-line Filter based on Modified-PCM-TLM Technique

---

E. Faghand<sup>1</sup>, E. Mehrshahi<sup>1</sup>, S. Karimian\*<sup>1</sup>, N. Karimian<sup>2</sup>

<sup>1</sup> School of Electrical Engineering, Shahid Beheshti University

<sup>2</sup> Department of Electrical and Electronic Engineering, The University of Manchester

*A new simple tool is proposed for design of multi-section coupled-line filters based on modified planar circuit method (M-PCM) and transmission line (TL) analysis, referred to as MPCM-TLM. Due to its fundamentally simple architecture, the presented tool offers significantly faster design and optimisation of coupled-line filters - for exactly the same initial simulation set-up - than other costly commercially-available tools (particularly at higher orders), giving equally reliable results. Validity and accuracy of the proposed tool has been verified through design of 3<sup>rd</sup>, 5<sup>th</sup> and 7<sup>th</sup> order coupled-line filters and comparative analysis between results obtained from the adopted approach and the HFSS. A remarkable 60% optimization time reduction is recorded in the case of 7<sup>th</sup> order filter using the proposed tool, for almost identical results to HFSS. Therefore, it can be confidently claimed that the proposed technique can be used as a reliable alternative to other complex, costly, processor-intensive CAD tools.*

*Keywords: Couplicator, Coupled-line Filter, Multi-section, Planar circuit analysis, segmentation, desegmentation.*

\* Corresponding author: S. Karimian; email:  
S\_Karimian@sbu.ac.ir;

## I. INTRODUCTION

The concept of planar circuit analysis was first introduced by [1, 2] as a method for analysing two-dimensional microwave integrated circuits. In general, for an  $N$ -port planar circuit, when port locations are specified, the impedance matrix of a planar circuit can be obtained using three methods; (a) Green's function for planar circuits with regular geometrical shapes [3], (b) Numerical techniques such as the contour integral method for completely arbitrary shapes, and (c) Segmentation and desegmentation methods, or more generally known as the planar circuit method (PCM), for analysis of composites of regular and arbitrary shapes. The latter is adopted in this work. Reports show that a variety of devices have been analysed using PCM, including rectangular waveguides [4], substrate integrated waveguides (SIW) [5], and active antennas [6]. However, to the best of authors' knowledge, no report has been published to illustrate the use of PCM in analysis and design of planar multi-section coupled-line filters. To this end, a new simple and very reliable tool is proposed based on the analysis provided in the present paper. The analysis relies on development of the so-called modified-PCM in an attempt to design  $N$ -port coupled lines using desegmentation method, and extending this to multi-section coupled-lines using segmentation method. Appropriate relations are also developed and given in Section II. As is demonstrated, the tool owes its simplicity and fast rendering to adoption of transmission line (TL) analysis within its core module, making it super flexible in transforming from single-section to multi-section coupled-lines. Validity and accuracy of the proposed technique are examined and confirmed against commercially-available simulators such as HFSS in Section III, for 3<sup>rd</sup>, 5<sup>th</sup> and 7<sup>th</sup> order coupled-line bandpass filters with appropriate simulation and measurement results. Finally, conclusions are drawn in Section IV.

## II. COUPLED-LINE DESIGN USING MODIFIED-PCM AND TLM

Choosing the most suitable method for analysing planar circuits mainly depends on the level of complexity of computations involved. For example, Green's function is used for simple geometries such as rectangle, triangle or circle, to give the voltage at any point on the planar circuit for a unit current source excitation elsewhere [7]. Here, modified planar circuit method (MPCM) is used in the form of segmentation and desegmentation techniques (Appendix A) to form and analyse a pair of coupled lines. This is then further extended to design of coupled-line filters as shall be seen.

### A. Coupled-line design using modified-PCM

The idea presented here is that, assuming two concentric rectangles  $\gamma$  and  $\beta$ , a coupled-line structure can be formed if the inner rectangle ( $\beta$ -circuit) is extruded longitudinally from either

side of the outer one ( $\gamma$ -circuit). Therefore, by adjusting port localization, and thereby modifying the planar circuit method (PCM), coupled lines can be created and analysed using desegmentation of two rectangular patches  $\alpha$  and  $\beta$ , as depicted in Fig. 1(a); where  $P_a$  and  $P_b$  represent input and output ports on  $\alpha$  and  $\beta$ . Similarly,  $C$  and  $D$  denote common (red) ports on the interface between  $\alpha$  and  $\beta$ , and (green) ports in the middle of  $\beta$ , respectively. The resulting coupled line is designed on Rogers RO4003 substrate with  $\epsilon_r = 3.55$  and thickness  $h = 1.6\text{mm}$ , and analysed using the modified-PCM. The results are plotted against those obtained from the commercially available full-wave software, HFSS, as illustrated in Fig. 1. As seen, a very good agreement is evident between the results, for different spacing values ( $S_1$  and  $S_2$ ) (see Fig. 1(b)); hence validating the modified-PCM technique to design coupled-line structures.

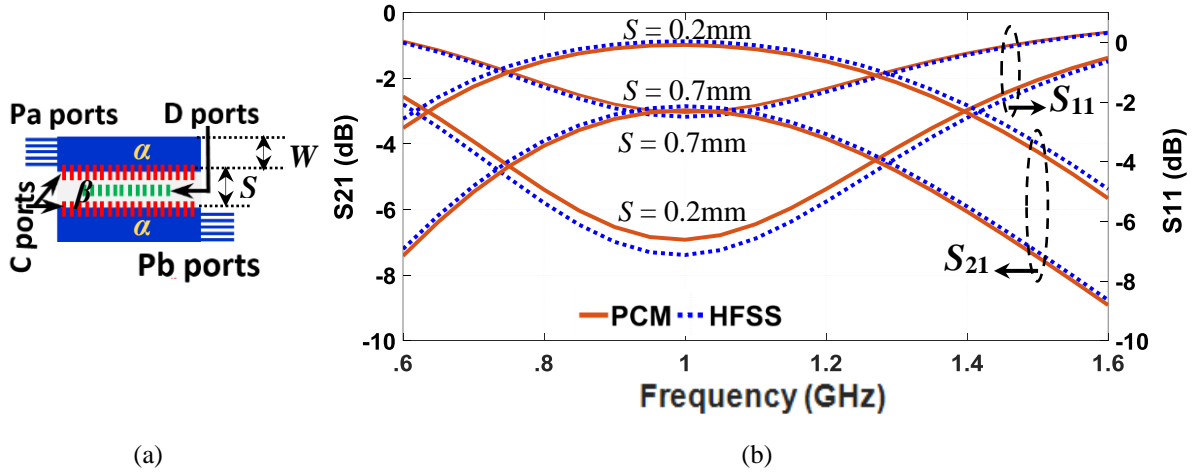


Fig. 1. (a) Illustration of coupled lines made by desegmentation of two planar rectangular patches,  $W$  (line width of rectangular patch) =  $1.5\text{mm}$ ,  $L$  (line length of rectangular patch) =  $48\text{mm}$ ; and (b) S-parameters plot of the coupled-line structure obtained by PCM and HFSS for two different spacing values ( $S_1 = 0.2\text{mm}$  and  $S_2 = 0.7\text{mm}$ ) between adjacent planar rectangular patches.

Multi-section coupled-line structure can be designed by connecting coupled-line pairs using segmentation process (see Fig. 2(a)). This requires calculating impedance matrix of every coupled line separately using desegmentation relation (A6), and then linking up rectangles using semengation relation (A4). Evidently, design of multi-section coupled-lines in commercially-available software (be it ADS, HFSS, CST, etc.) is an iterative process and involves complex, processor-intensive and time-consuming optimisations. In this paper a new approach is presented, which is manifested in the form an open-source tool, that significantly reduces such complexity. As shall be explained in the following section, the proposed tool is based on simultaneously utilizing the modified-PCM and impedance calculations of single coupled-line section. Relying on simple, fast and accurate lumped-element equivalent circuit analysis, equivalent circuit lumped element values are calculated and optimum associated coupled-line geometric parameters are generated, producing the final design layout very quickly.

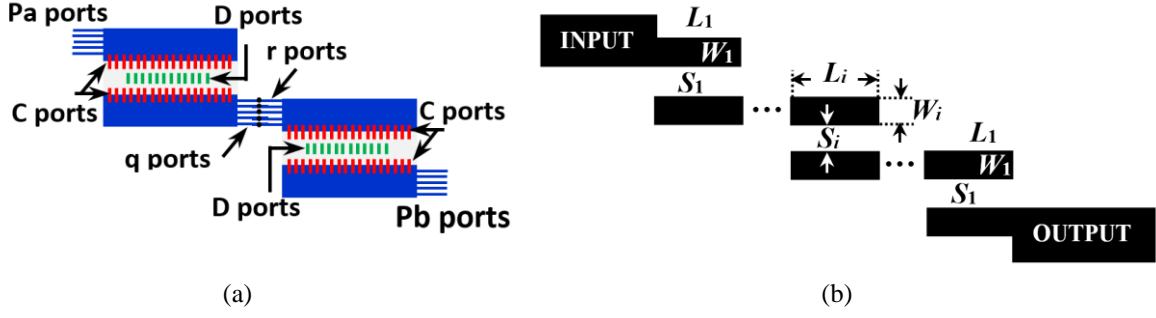


Fig. 2. (a) Equivalent bi-section planar circuit model (with  $N$  ports), and (b) layout of cascaded multi-conductor coupled-line structure.

## B. Extracting equivalent circuit values using TLM

Figure 3(a) depicts structure of a simple two-conductor coupled-line with line width,  $W$ , spacing between two lines,  $S$ , length of coupled lines,  $l$ . Equivalent circuit model of this coupled-line for an infinitesimal line section  $\Delta z$  is shown in Fig. 3(b); where  $L$ ,  $C$ ,  $R$  and  $G$  are per-unit-length inductance, capacitance, resistance and conductances, respectively. Also,  $L_m$  and  $C_m$  represent mutual coupling inductance and capacitance, respectively.

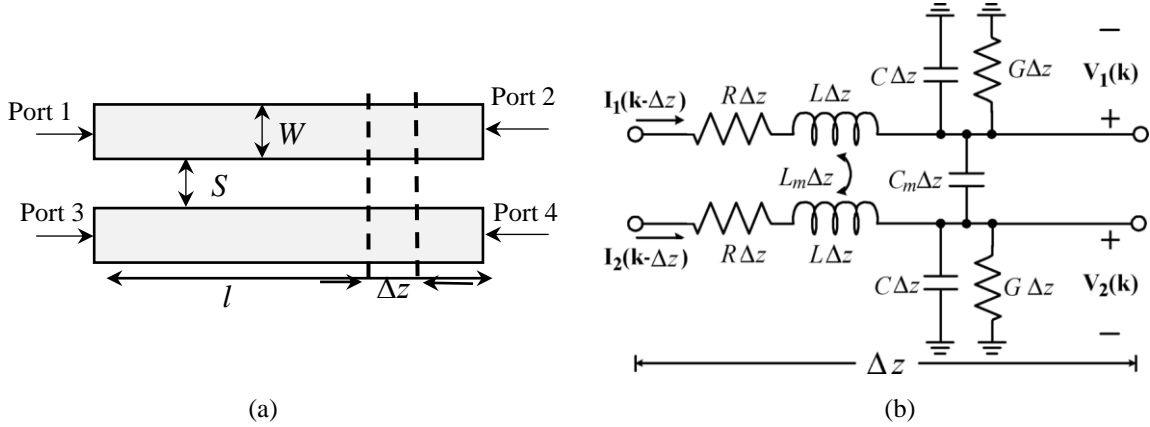


Fig. 3. (a) Layout and (b) equivalent circuit model of a two-conductor coupled-line.

Assuming a lossless line, impedance ( $Z$ ) and admittance ( $Y$ ) matrices of the coupled line of Fig. 3(a) can be given as:

$$Z = \begin{bmatrix} jL\omega & jL_m\omega \\ jL_m\omega & jL\omega \end{bmatrix} \quad (1)$$

$$Y = \begin{bmatrix} j(C + C_m)\omega & -jC_m\omega \\ -jC_m\omega & j(C + C_m)\omega \end{bmatrix} \quad (2)$$

where  $\omega$  is the angular frequency.

For the coupled line, the Telegrapher's Equations can result in input and output voltages and currents ( $V_1, I_1$  and  $V_2, I_2$ ) of:

$$\begin{bmatrix} V_1 \\ V_2 \end{bmatrix} = a_1^+ (e^{-j\beta_1 x} + \Gamma_1 e^{j\beta_1 x}) \begin{bmatrix} 1 \\ 1 \end{bmatrix} + a_2^+ (e^{-j\beta_2 x} + \Gamma_2 e^{j\beta_2 x}) \begin{bmatrix} 1 \\ -1 \end{bmatrix} \quad (3)$$

$$\begin{bmatrix} I_1 \\ I_2 \end{bmatrix} = \frac{a_1^+ \beta_1}{(L + L_m) \omega} (e^{-j\beta_1 x} - \Gamma_1 e^{j\beta_1 x}) \begin{bmatrix} 1 \\ 1 \end{bmatrix} + \frac{a_2^+ \beta_2}{(L - L_m) \omega} (e^{-j\beta_2 x} - \Gamma_2 e^{j\beta_2 x}) \begin{bmatrix} 1 \\ -1 \end{bmatrix} \quad (4)$$

Using (3) and (4), phase constant  $\beta$  can be obtained as:

$$\beta_1 = \omega \sqrt{C(L + L_m)} \quad (5)$$

$$\beta_1 = \omega \sqrt{(C + 2C_m)(L - L_m)} \quad (6)$$

Considering the boundary condition and symmetry of impedance matrix by substituting  $\beta$  in voltage and current relations, four main elements of impedance matrices  $Z$  of a lossless coupled line can be given as:

$$Z_{11} = \frac{\sqrt{\frac{L + L_m}{C}} * \cos \beta_1 l * \sin \beta_2 l + \sqrt{\frac{L - L_m}{C + 2 * C_m}} * \sin \beta_1 l * \cos \beta_2 l}{2j * \sin \beta_1 l * \sin \beta_2 l} \quad (7)$$

$$Z_{21} = \frac{\sqrt{\frac{L + L_m}{C}} * \cos \beta_1 l * \sin \beta_2 l - \sqrt{\frac{L - L_m}{C + 2 * C_m}} * \sin \beta_1 l * \cos \beta_2 l}{2j * \sin \beta_1 l * \sin \beta_2 l} \quad (8)$$

$$Z_{31} = \frac{\sqrt{\frac{L + L_m}{C}} * \sin \beta_2 l + \sqrt{\frac{L - L_m}{C + 2 * C_m}} * \sin \beta_1 l}{2j * \sin \beta_1 l * \sin \beta_2 l} \quad (9)$$

$$Z_{41} = \frac{\sqrt{\frac{L + L_m}{C}} * \sin \beta_2 l - \sqrt{\frac{L - L_m}{C + 2 * C_m}} * \sin \beta_1 l}{2j * \sin \beta_1 l * \sin \beta_2 l} \quad (10)$$

$$Z = \begin{bmatrix} Z_{11} & \cdots & Z_{14} \\ \vdots & \ddots & \vdots \\ Z_{41} & \cdots & Z_{44} \end{bmatrix} \quad (11)$$

where (11) is the  $Z$  matrix of the coupled line under the symmetry, reciprocity and unitary conditions.

The impedance matrix  $Z$  of the coupled line can be determined using (7)-(10) if the equivalent circuit parameters  $L$ ,  $C$ ,  $L_m$  and  $C_m$  are known. However, since these parameters are all unknown for start, the impedance matrix  $Z$  obtained from the modified-PCM analysis given in (A6) is substituted in relations (7)-(10) obtained from equivalent circuit analysis, to solve four simultaneous equations (using the Gradient method) and to extract the four unknowns  $L$ ,  $C$ ,  $L_m$  and  $C_m$ .

To verify the validity of the proposed method, the coupled-line designed using modified-PCM (seen in Fig. 1) is assumed on Rogers RO4003 substrate ( $h = 0.25\text{mm}$ ,  $\epsilon_r = 3.55$ ,  $\text{TanD} = 0.0027$ ), with line width  $W = 1.5$ , spacing  $S = 0.8$ , and length  $l = 48$  (all in mm). Utilizing (A6), and (7)-(10), the lumped element values associated to the specified geometries are determined to be,  $L = 432.55\text{nH}$ ,  $C = 42.86\text{pF}$ ,  $L_m = 125.37\text{nH}$ , and  $C_m = 12.15\text{pF}$ . As such, relevant S-parameters are produced by simple Z-to-S conversion. The same geometry is also analysed in the full-wave simulator ANSYS HFSS in order to compare the results with the presented method.

As depicted in Fig. 4, a very good match is evident between results obtained from HFSS and the proposed method; confirming the validity and accuracy of the proposed technique.

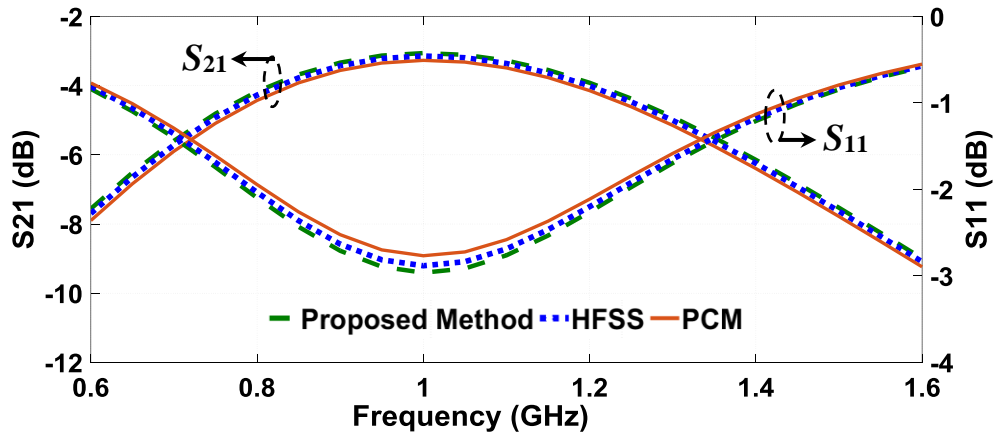


Fig. 4. S-parameters plot of the referred coupled-line structure obtained from the presented technique.

Regardless of the technique used, analysis of multi-section coupled-line structures becomes very complicated, be it using PCM, modified-PCM or well-known methods such as Moments or FEM; due to the large number of analytical ports involved (in PCM) (see Fig. 2(a)), meshing, and iteration frequency (in HFSS). However, the beauty of the proposed approach is that it is inherently simple, as the modified-PCM method is used once only at the beginning of the analysis, and that the rest of analysis relies on solving straight-forward simple TL equations; thus, offering the ability to rapidly generate the optimal layout. Therefore, the presented technique is extended to offer a simplified procedure for design of multi-section coupled-lines; where the analysis of the overall structure would involve analysis of individual coupled-line sections from (11).

In order to provide a comprehensive dataset for the developed tool, calculations have been carried out for a range of different values of  $S$  (assuming fixed  $50\Omega$  TLs), for which relevant  $L$ ,  $C$ ,  $L_m$  and  $C_m$  have been extracted and recorded in the form of a look-up table. Thus, for a coupled line with fixed line widths ( $50\Omega$ ), only the spacing  $S$  must be specified, according to which  $L$ ,  $C$ ,  $L_m$  and  $C_m$  are extracted immediately. Figure 5 is a graphical illustration of electrical versus physical

parameters of the coupled-line analysed earlier in this paper, plotted from the look-up table. Note that limited data has been shown in the figure for illustration purposes only.

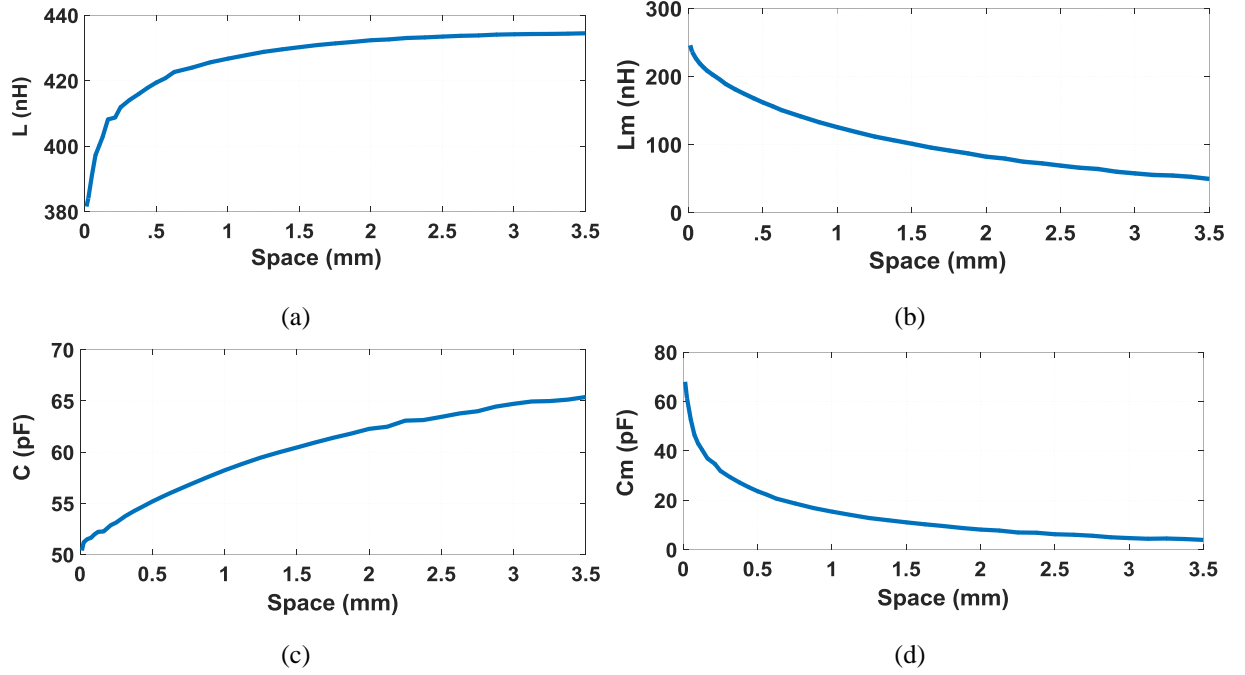


Fig. 5. Plot of change of  $L$ ,  $L_m$ ,  $C$ , and  $C_m$  change of  $S$  at 0.6-1.6 GHz for  $W = 1.5$ mm,  $L = 48$ mm on Rogers RO4003 with  $\epsilon_r = 3.55$ , and  $h = 0.25$ mm.

Evidently, such information can be very useful in that for any desired spacing, associated lumped-element values ( $L$ ,  $C$ ,  $L_m$ , and  $C_m$ ) can be extracted immediately, and vice versa. The data becomes particularly useful if more than one pair of coupled-line section (a multi-section coupled-line) is present; since the same procedure can be applied to the other pairs of coupled-line structure too (assuming minimum or no mutual coupling between pairs of coupled-line). These extracted lumped-element values can be substituted in (7)-(10), yielding in  $Z$  matrix (relation (11)) for each coupled-line section. The  $Z$  matrices shall be converted into ABCD matrices, then multiplied, to result the overall  $Z$  matrix (and eventually the  $S$ -parameters) of the multi-conductor coupled-line.

### III. DESIGN OF MULTI-SECTION COUPLED-LINE FILTER

Here, multi-section coupled-line filters are designed based on the analysis provided so far. The flowchart of Fig. 6 illustrates the proposed design procedure graphically in order to simplify the design process.



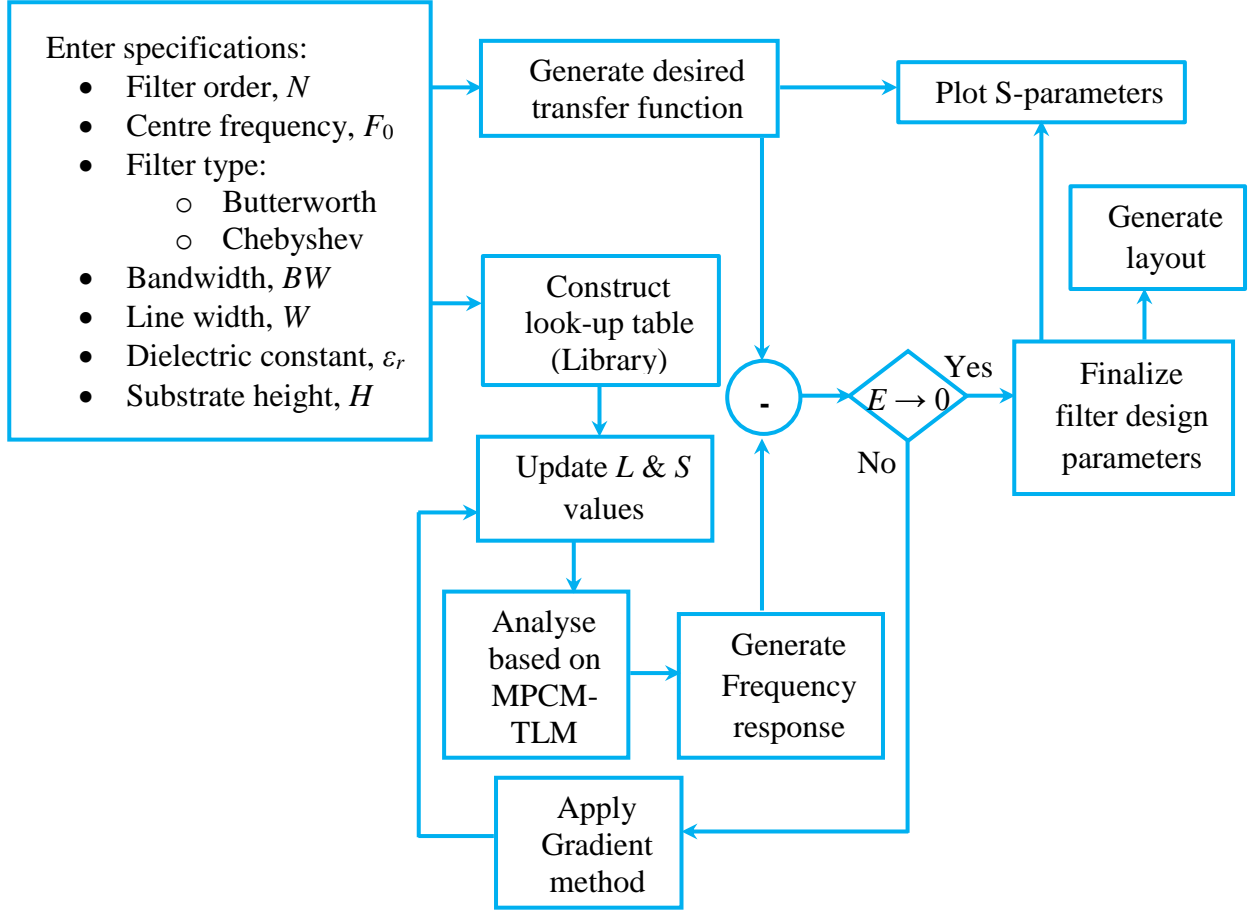


Fig. 6. Design procedure for the proposed multi-section coupled-line filter.

As is seen, one should enter filter specifications including desired frequency response (filter type, filter order,  $N$ , centre frequency  $F_0$ , bandwidth,  $BW$ ) and substrate parameters (TL widths  $W$ , substrate height  $H$ , and relative dielectric constant,  $\epsilon_r$ ). A customized look-up table (or so-called library) is constructed accordingly, from which optimum TL length  $L$  ( $\lambda/4$  at  $F_0$ ) and spacing  $S$  are chosen, to generate a frequency response based on the proposed method. The generated response is then compared to the desired transfer function, producing an error difference,  $E$ . If  $E \rightarrow 0$  is satisfied, final physical parameters are produced based on which filter layout is generated and S-parameters are plotted. However, if  $E \rightarrow 0$  is not satisfied, the Gradient method is applied in an iterative process to generate updated  $L$  and  $S$  values, producing closer-to-desired frequency responses until the condition is met; eventually offering an optimal filter layout. Screenshot of the developed tool for 5<sup>th</sup> order coupled-line bandpass filter is illustrated in Fig. 7.

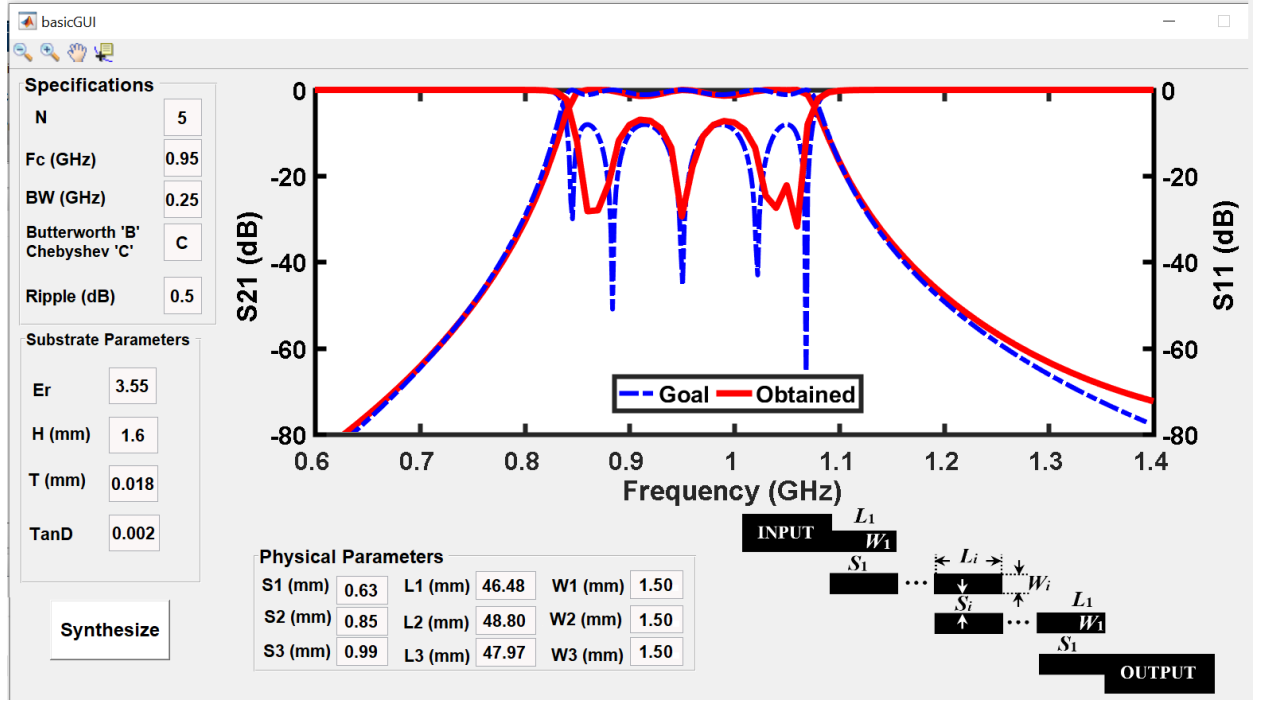
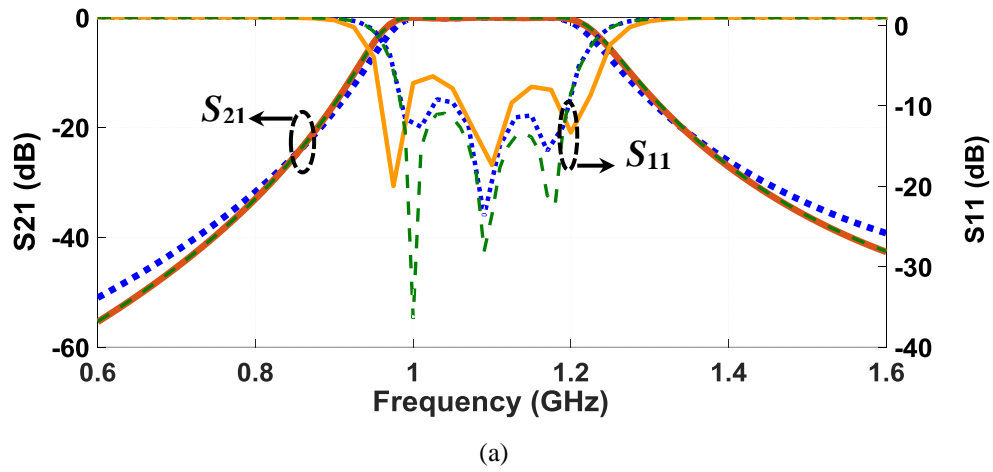
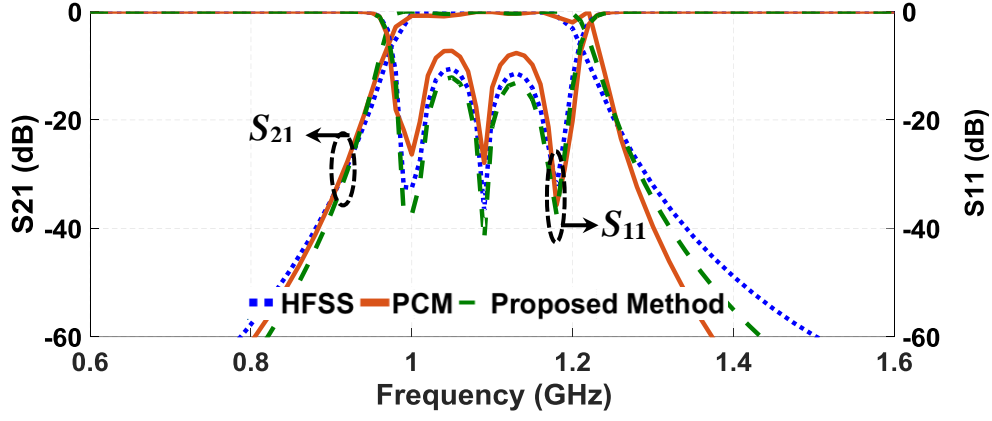


Fig. 7. Screenshot of the developed tool for the case of 5<sup>th</sup> order coupled-line bandpass filter.

The final section of this paper takes a step further to validate the proposed technique, by designing 3<sup>rd</sup>, 5<sup>th</sup> and 7<sup>th</sup> order multi-section coupled-line filters on different substrates, and compare the results against those obtained from HFSS and PCM. . Moreover, the 7<sup>th</sup> order coupled-line filter, which is designed using the proposed tool for direct broadcast satellite (DBS) applications, is fabricated. Figure 8 compares S-parameter results for (a) 3<sup>rd</sup> order and (b) 5<sup>th</sup> order coupled-line filters designed on Arlon AD255A ( $\epsilon_r = 2.54$ ,  $h = 1.6\text{mm}$ ,  $TanD = 0.0015$ ), and Taconic TLT ( $\epsilon_r = 2.54$ ,  $h = 1.6\text{mm}$ ,  $TanD = 0.0006$ ), respectively. Evidently, in both cases the results obtained from the proposed method match very closely with those obtained from HFSS.

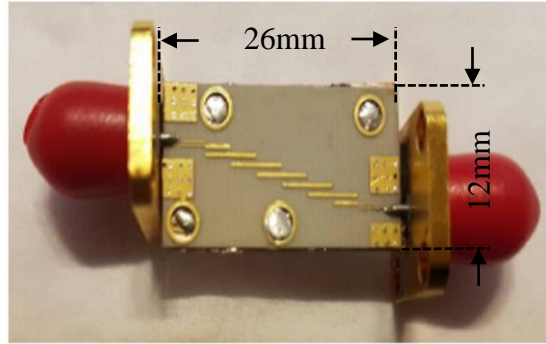




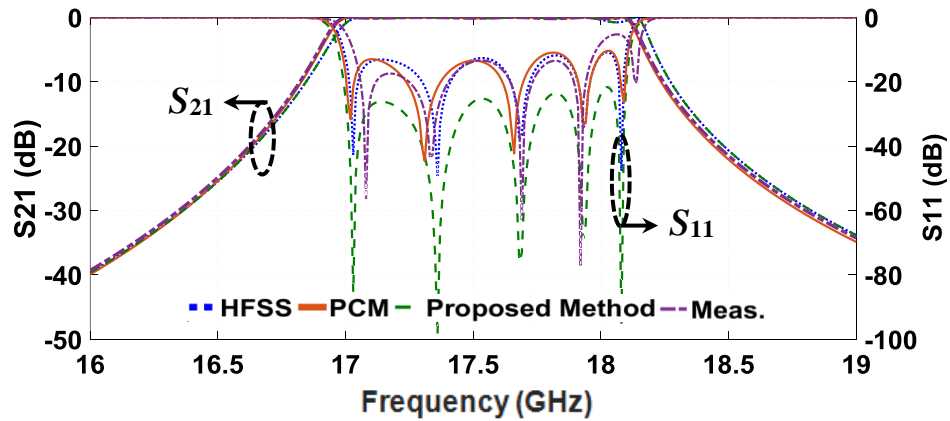
(b)

Fig. 8. S-parameters of (a) 3<sup>rd</sup> order coupled-line filter ( $W_1 = 1.5$ ,  $W_2 = 1.9$ ,  $L_1 = L_2 = 48$ ,  $S_1 = 0.4$ ,  $S_2 = 0.8$ ), and (b) 5<sup>th</sup> order coupled-line filter ( $W_1 = 1.6$ ,  $W_2 = 2$ ,  $W_3 = 2$ ,  $L_1 = L_2 = L_3 = 48$ ,  $S_1 = 0.4$ ,  $S_2 = 0.8$ ,  $S_3 = 1.25$ ), designed with PCM, ECMM and HFSS (all dimensions in mm).

Furthermore, the 7<sup>th</sup> order bandpass filter is designed based on the proposed technique and fabricated on Rogers RO4003 with  $\epsilon_r = 3.55$ ,  $h = 0.25\text{mm}$ ,  $\text{Tan}D = 0.0027$  (photograph seen in Fig. 9(a)). Measurement results of this filter are compared against those obtained from PCM, HFSS, and the proposed tool, as depicted in Figure 9(b). It is clear evidence that the results are all in very good agreement and thus, it is a solid validation of the functioning and accuracy proposed approach.



(a)



(b)

Fig. 9. (a) Photograph of the 7<sup>th</sup> order fabricated filter, and (b) its S-Parameter response; ( $W_1 = 0.17$ ,  $W_2 = 0.2$ ,  $W_3 = 0.2$ ,  $W_4 = 0.2$ ,  $L_1 = 2.58$ ,  $L_2 = L_3 = L_4 = 2.54$ ,  $S_1 = 0.12$ ,  $S_2 = 0.3$ ,  $S_3 = 0.32$ ,  $S_4 = 0.4$ ) (all in mm).

To complete the comprehensive analysis presented in this paper, optimisation times for design of single coupled-line, and 3<sup>rd</sup>, 5<sup>th</sup> and 7<sup>th</sup> order filters based on PCM, HFSS and the proposed technique are recorded and compared in Table I. Evidently, for exactly the same initial simulation set-up (i.e. meshing, steps, etc.), simplicity of the proposed technique has manifested itself in minimum time consumption in the optimization process. This is a significant advantage particularly for design of higher order filters, where for instance in the case of 7<sup>th</sup> order filter, almost 60% optimization time reduction is recorded for obtaining almost the same results, which is a remarkable achievement.

Therefore, it can be safely claimed that the technique proposed in this paper is by far superior to other popular techniques for being simpler and faster in simulation and optimization, and so, can be used as a reliable alternative to those techniques. This is particularly thanks to the use of TL (hence, equivalent circuit model) analysis, enabling extendibility of such analysis to other multiport multi-section structures such as filters (or any device formed by coupled-lines); unlike in PCM where complexity increases hugely as number of ports increase, or in HFSS where increases in mesh number significantly adds to the complexity of structural analysis.

Table I. Recorded optimization duration in filter design (all in seconds).

Filter design technique	One coupled-line	3 <sup>rd</sup> order	5 <sup>th</sup> order	7 <sup>th</sup> order
PCM	50	180	300	360
HFSS	60	240	330	460
MPCM-TLM ( <b>This work</b> )	40	100	120	150

#### IV. CONCLUSION

In this paper a new technique is presented for analysis and design of coupled-lines and multi-conductor structures made of coupled-lines (such as coupled-line filters) which takes advantage of modified-PCM and TL analysis, to offer a tool by far a simpler and faster optimisation alternative to existing commercially available tools. It has been confirmed throughout the paper that for exactly the same initial simulation set-up (i.e. meshing, steps, etc.), almost identical results have been obtained from the proposed technique and the commercially-available tools such as HFSS. The simplicity of the proposed technique has manifested itself in minimum time consumption in the optimization process. This is a significant advantage particularly for design

of higher order filters, where for instance in the 7<sup>th</sup> order filter, almost 60% optimization time reduction is recorded for obtaining almost the same results, which is a remarkable achievement. This is particularly thanks to the use of TL (hence equivalent circuit model) analysis, enabling extendibility of such analysis to other multiport multi-conductors such as wide range of filters (or any device formed by coupled-lines); unlike in PCM where complexity increases hugely as number of ports increase, or in HFSS where increases mesh number significantly adds to the complexity of structural analysis.

## REFERENCES

- [1] T. Okoshi, "Microwave planar circuits," *Rep. Tech. Group. Inst. Electron. Commun. Eng. Jpn.* Pap. MW68-69, Feb. 17. 1969.
- [2] T. Okoshi, "Microwave planar circuits," *Rec. Jt. Nat. Conv. Four EE Inst.*, Pap. No. 1468. Mar. 1969.
- [3] T. Okoshi and T. Miyoshi, "The planar circuit-An approach to microwave integrated circuitry," *IEEE Trans. Microwave Theory Tech.*, vol. MTT-20, pp. 245-252. Apr. 1972.
- [4] J. A. Encinar, Changhua Wan and J. R. Mosig, "Generalized scattering matrix computation of the transition: microstrip line-rectangular waveguide, as a building block for the analysis of multilayer microstrip circuits and antennas," *IEEE Antennas and Propagation Society International Symposium*, 1997. Digest, Montreal, Quebec, Canada, 1997, pp. 626-629 vol.2.
- [5] M. Kishihara, K. Yamane and I. Ohta, "Analysis of Post-Wall Waveguide by H-Plane Planar Circuit Approach," *2007 IEEE/MTT-S International Microwave Symposium*, Honolulu, HI, 2007, pp. 1931-1934.
- [6] H. Rogier, D. De Zutter, B. De Mulder and J. Vandewege, "Design of active planar antennas based on circuit/full-wave co-optimization," *IEEE Antennas and Propagation Society Symposium*, 2004, Monterey, CA, USA, 2004, pp. 2329-2332 Vol.3.
- [7] T. Okoshi and T. Miyoshi, "The Planar Circuit – An approach to microwave integrated circuit," *IEEE Trans. Microwave Theory Tech.*, vol. MTT-20, pp.245-252. Apr. 1972.
- [8] T. Itoh, *Numerical Techniques for Microwave and Milimeter-Wave Passive Structures*. New York: Wiley, 1988.
- [9] T. Okoshi and T. Miyoshi, "The planar circuit-An approach to microwave integrated circuitry," *IEEE Trans. Microwave Theory Tech.*, vol. MTT-20, pp. 245-252. Apr. 1972.
- [10] T. Okoshi, *Planar Circuits for Microwave and Lightwave*. Springer-Verlag, New York, 1985.
- [11] P. C. Sharma and K. C. Gupta, "An alternative procedure for implementing desegmentation method," *IEEE Trans. Microwave Theory Tech.*, vol. MTT-32, pp. 1-4, Jan. 1984.

## ANNEX I. PLANAR CIRCUIT ANALYSIS USING SEGMENTATION AND DESEGMENTATION METHODS

In this section, segmentation and desegmentation techniques are briefly overviewed; to be used in analysis of pair of coupled lines and eventually, design of coupled line filters in this paper. Figure A1 depicts an  $N$ -port planar circuit of arbitrary shape. Different ports can be defined along the periphery of this circuit with port widths of say  $w_i$  and  $w_j$ . The rest of the periphery is either open, shorted or terminated by an impedance wall [8].

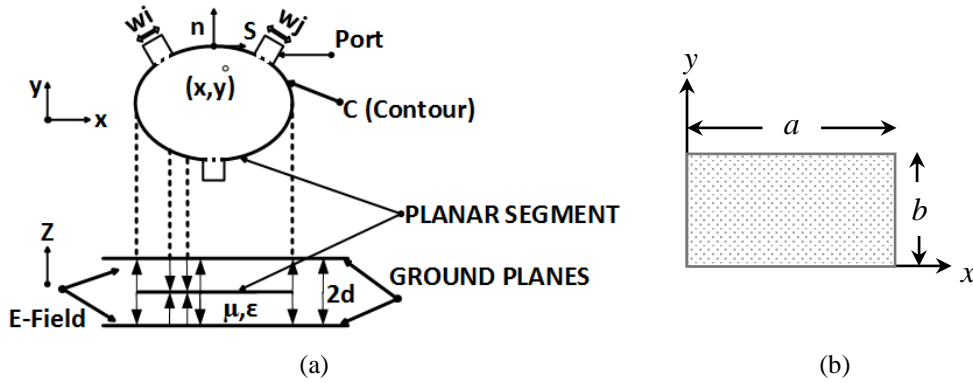


Fig. A1. (a) A triplate-type planar circuit, (b) rectangular patch whose green's function is given in (2) [8].

When port locations are specified, the impedance matrix  $Z_{ij}$  characterising the planar component can then be easily derived using the Green's function, in (A1).

$$Z_{ij} = \sum_j \frac{1}{pw_i w_j} \int_0^{w_i} \int_0^{w_j} G(s | s_0) ds ds_0 \quad (A1)$$

where  $G(s|s_0)$  is the Green's function, and  $p$  is constant ( $p = 1$  for stripline and  $p = 2$  for microstrip transmission line).

In Fig. A1(b), for a simple rectangular patch with the form of either  $\gamma$  or  $\beta$ , Green's function can be defined as:

$$G(x, y | x_0, y_0) = \frac{j\omega\mu d}{ab} \sum_{n=0}^{\infty} \sum_{m=0}^{\infty} \frac{\sigma_m \sigma_n \cos(k_x x_0) \cos(k_y y_0) \cos(k_x x) \cos(k_y y)}{k_x^2 + k_y^2 - k_0^2} \quad (A2)$$

where  $x$  and  $y$  are excitation points, and  $x_0$  and  $y_0$  are arbitrary observation points,  $\mu$ : permeability,  $a$ : patch length,  $b$ : patch width,  $\sigma$  is a constant with  $\sigma_i = 1$  (if  $i = 0$ ), and  $\sigma_i = 2$  (if  $i \neq 0$ ), and  $k_x = m\pi/a$  and  $k_y = n\pi/b$ .

## A) Segmentation Method

The segmentation method, which was first introduced by [7], is a planar procedure for network analysis of two-dimensional microwave circuits [9, 10]. It involves dividing a complex planar circuit into simple parts that have regular shapes whose general characteristic, impedance function and Green's function are known. Therefore, the impedance function and so the scattering matrix of the entire structure made of simple parts can be easily obtained. Such analysis requires assigning a number of ports to the overall structure and its constituent parts (see rectangular patches A and B in Fig. A2). The number of these ports depends on the common region interface [11]. In Fig. A2,  $P_{ai}$  and  $P_{bi}$  are input and output ports, and  $q_i$  and  $r_i$  ( $i = 1, 2, 3, \dots, n$ ) are the number of intermediate ports, respectively.

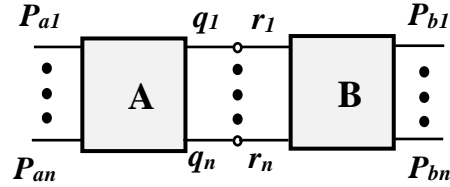


Fig. A2. Representation of an  $N$ -port planar circuit adopted in the segmentation analysis.

In general, the relation between voltages and currents on different ports can be derived as:

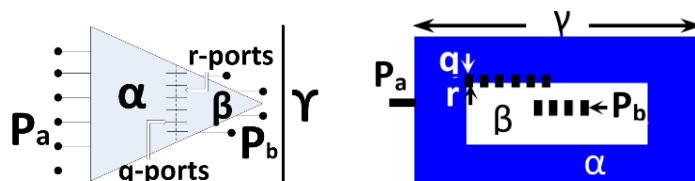
$$\begin{bmatrix} V_p \\ V_q \\ V_r \end{bmatrix} = \begin{bmatrix} Z_{pp} & Z_{pq} & Z_{pr} \\ Z_{qp} & Z_{qq} & Z_{qr} \\ Z_{rp} & Z_{rq} & Z_{rr} \end{bmatrix} \begin{bmatrix} i_p \\ i_q \\ i_r \end{bmatrix} \quad (A3)$$

where  $Z_{pp}$  is impedance relation between all  $p$  ports (i.e. all  $P_{ai}$  and  $P_{bi}$  ports),  $Z_{pq}$  is impedance relation between all  $P_{ai}$  and  $q$  ports,  $Z_{pr}$  is impedance relation between all  $P_{bi}$  and  $r$  ports, and so on. Using the boundary condition  $V_q = V_r$  and  $i_q = -i_r$  in intermediate ports, Equation (A3) can be solved and the total impedance  $Z_{AB}$  is obtained as [11]:

$$Z_{AB} = Z_{pp} + (Z_{pq} - Z_{pr}) * (Z_{qq} + Z_{rr} - Z_{qr} - Z_{rq})^{-1} * (-Z_{qp} + Z_{rp}) \quad (A4)$$

## B) Desegmentation Method

Desegmentation method is used for irregular structures (e.g. shapes of Fig. A3), whose Green's function is not available, and so cannot be analysed simply by the segmentation method.



(a) (b)  
Fig. A3. Examples of desegmented planar circuits [11].

In the case of example of Fig. A3(a), impedance matrix of the trapezoid  $\alpha$  can be obtained by adding a small triangle  $\beta$  to it, to form the larger triangle  $\gamma$ . So, by establishing the impedance matrices of triangles  $\beta$  and  $\gamma$  with known Green's functions, the impedance matrix of the trapezoid can be obtained. The same is true for Fig. A3(b), where the rectangular blue doughnut-shape  $\alpha$  can be obtained when  $\beta$  and  $\gamma$  are known. Besides, the relation between Z-matrices of the three shapes is obtained when three sets of discrete ports are defined on the inner and outer interfaces, i.e. port  $P_a$  on the outside of  $\gamma$ , port  $P_b$  inside  $\beta$ , and intermediate ports  $q$  and  $r$ , on the border between  $\alpha$  and  $\beta$ . The number of intermediate ports depends on the field changes along the interface. Let the currents of the ports be  $I_q$ ,  $I_r$ ,  $I_{pa}$  and  $I_{pb}$ , and the voltages equal to  $V_q$ ,  $V_r$ ,  $V_{pa}$ , and  $V_{pb}$ ; and assuming that  $q = r$ , the boundary conditions are considered as  $V_q = V_r$  and  $I_q = -I_r$ . Thus, using (A1)-(A2), impedance matrices  $Z_\alpha$ ,  $Z_\beta$  and  $Z_\gamma$  can be defined as [11]:

$$Z_\alpha = \begin{bmatrix} Z_{p_a\alpha} & Z_{p_aq} \\ Z_{qp_a} & Z_{qq} \end{bmatrix}, Z_\beta = \begin{bmatrix} Z_{rr} & Z_{rp_b} \\ Z_{p_b r} & Z_{p_b\beta} \end{bmatrix}, Z_\gamma = \begin{bmatrix} Z_{p_a\gamma} & Z_{p_a p_b} \\ Z_{p_b p_a} & Z_{p_b\gamma} \end{bmatrix} \quad (A5)$$

Given the matrix elements  $\beta$  and  $\gamma$ , and using the PCM analysis, elements of the matrix can be obtained from (A6) [8].

$$Z_\alpha = \begin{bmatrix} Z_{p_a\gamma} - Z_{p_a p_b} \left[ Z_{p_b\gamma} - Z_{p_b\beta} \right]^{-1} Z_{p_b p_a} & -Z_{p_a p_b} \left[ Z_{p_b\gamma} - Z_{p_b\beta} \right]^{-1} Z_{p_b r} \\ -Z_{r p_b} \left[ Z_{p_b\gamma} - Z_{p_b\beta} \right]^{-1} Z_{p_b p_a} & -Z_{rr} - Z_{r p_b} \left[ Z_{p_b\gamma} - Z_{p_b\beta} \right]^{-1} Z_{p_b r} \end{bmatrix} \quad (A6)$$

Therefore, the impedance matrix  $Z_\alpha$  of the extracted shape (i.e.  $\alpha$ ) of Fig. A3(b) has been generated whose elements are port impedances.

## Bibliographies



**Elahe Faghand** was born in Iran, in 1992. She received her B.S. from Shahed University and M.S. degree in electrical engineering from Shahid Beheshti University of Tehran, respectively, in 2015 and 2017. She is currently research assistant in the Department of Electrical Engineering at the Shahid Beheshti University.





**Dr Esfandiar Mehrshahi** was born in Tehran, Iran 1964. He received his B.Sc. from Iran University of Science and Technology, Tehran, Iran, in 1987, and the M.Sc. and Ph.D. degrees from Sharif University of Technology, Tehran, Iran, in 1991 and 1998, respectively. Since 1990 he has been involved in several research and engineering projects at the Iran Telecommunications Research Centre (ITRC). He is currently an Associate Professor at Shahid Beheshti University, Tehran, Iran. His main areas of interest are non-linear simulation of microwave circuits and microwave oscillator's spectrum.



**Dr Shokrollah Karimian** is an Assistant Professor in School of Electrical Engineering at Shahid Beheshti University. As a member of IEEE, with over 50 publications, he has made valuable contribution to the RF and microwave/mm-wave community.

Noushin Karimian received the Ph.D. degree in Electrical and Electronic Engineering from The University of Manchester, Manchester, U.K., in 2014. Since then, she has been a Research Associate with University of Manchester on various international projects. She is a coauthor of more than 40 international conference and journal papers and has a registered patent. Her main research interests include electromagnetic sensors for NDT applications and digital signal processing. Dr. Karimian has been actively involved both as technical and organizational committee member of international conferences, and most recently the European Microwave Conference. She is a member of IEEE, IET, EuMA, BINDT, and IOP. She is currently acting as the Treasurer for the IEEE U.K. and Ireland Section, and a committee member of The University of Manchester IEEE Student Branch. She is also a committee member of the IEEE U.K. and Ireland Women in Engineering.

## List of figures and tables

Fig. 1. (a) Illustration of coupled lines made by desegmentation of two planar rectangular patches,  $W$  (line width of rectangular patch) = 1.5mm,  $L$  (line length of rectangular patch) = 48mm; and (b) S-parameters plot of the coupled-line structure obtained by PCM and HFSS for two different spacing values ( $S_1 = 0.2\text{mm}$  and  $S_2 = 0.7\text{mm}$ ) between adjacent planar rectangular patches.

Fig. 2. (a) Equivalent bi-section planar circuit model (with  $N$  ports), and (b) layout of cascaded multi-conductor coupled-line structure.

Fig. 3. (a) Layout and (b) equivalent circuit model of a two-conductor coupled-line.

Fig. 4. S-parameters plot of the referred coupled-line structure obtained from the presented technique.

Fig. 5. Plot of change of  $L$ ,  $L_m$ ,  $C$ , and  $C_m$  change of  $S$  at 0.6-1.6 GHz for  $W = 1.5\text{mm}$ ,  $L = 48\text{mm}$  on Rogers RO4003 with  $\epsilon_r = 3.55$ , and  $h = 0.25\text{mm}$ .

Fig. 6. Design procedure for the proposed multi-section coupled-line filter.

Fig. 7. Screenshot of the developed tool for the case of 5<sup>th</sup> order coupled-line bandpass filter.

Fig. 8. S-parameters of (a) 3<sup>rd</sup> order coupled-line filter ( $W_1 = 1.5$ ,  $W_2 = 1.9$ ,  $L_1 = L_2 = 48$ ,  $S_1 = 0.4$ ,  $S_2 = 0.8$ ), and (b) 5<sup>th</sup> order coupled-line filter ( $W_1 = 1.6$ ,  $W_2 = 2$ ,  $W_3 = 2$ ,  $L_1 = L_2 = L_3 = 48$ ,  $S_1 = 0.4$ ,  $S_2 = 0.8$ ,  $S_3 = 1.25$ ), designed with PCM, ECMM and HFSS (all dimensions in mm).  
 Fig. 9. (a) Photograph of the 7<sup>th</sup> order fabricated filter, and (b) its S-Parameter response; ( $W_1 = 0.17$ ,  $W_2 = 0.2$ ,  $W_3 = 0.2$ ,  $W_4 = 0.2$ ,  $L_1 = 2.58$ ,  $L_2 = L_3 = L_4 = 2.54$ ,  $S_1 = 0.12$ ,  $S_2 = 0.3$ ,  $S_3 = 0.32$ ,  $S_4 = 0.4$ ) (all in mm).

Table I. Recorded optimization duration in filter design (all in seconds).